The Volcano Effect in Bacterial Chemotaxis

Julie E Simons[a,*], Paul A. Milewski[a]

[a]*Department of Mathematics, University of Wisconsin, Madison, 480 Lincoln Dr., Madison, WI 53706*

Abstract

A population-level model of bacterial chemotaxis is derived from a simple bacterial-level model of behavior. This model, to be contrasted with the Keller-Segel equations, exhibits behavior we refer to as the "volcano effect": steady-state bacterial aggregation forming a ring of higher density some distance away from an optimal environment. The model is derived, as in Erban and Othmer [7], from a transport equation in a state space including the internal biochemical variables of the bacteria and then simplified with a truncation at low moments with respect to these variables. We compare the solutions of the model to stochastic simulations of many bacteria, as well as the classic Keller-Segel model. This model captures behavior that the Keller-Segel model is unable to resolve, and sheds light on two different mechanisms that can cause a volcano effect.

Keywords: chemotaxis, stochastic, bacteria, swarming, Keller-Segel

1. Introduction

Chemotaxis refers to the process of a directed motion of organisms towards or away from a chemical gradient. This phenomenon has been described since the late nineteenth century and extensively studied in bacteria for the past fifty years. In observations of such bacterial behavior, populations spread in a coordinated manner, biased toward the direction of improving environmental conditions. In certain species, the individual bacteria in the swarm perform a biased simple random walk which take the form of what are known as "runs" and "tumbles". A bacteria will run or swim in one direction, and then stop and tumble for a short period of time, allowing it to reorient and then swim in a new, randomly chosen direction. This motion is accomplished by flagellar motors, which propel a bacterium forward during a run and are considered effectively turned off during a tumble. The bias in this process comes from the chemotactic sensing ability, which, during each swim, decreases the probability

*Corresponding author

Email addresses: simons@math.wisc.edu (Julie E Simons), milewski@math.wisc.edu (Paul A. Milewski)

of the bacteria entering into a tumbling state if the environment is improving and increases it if its environment is deteriorating.

The chemotactic sensory system is commonly described as an excitation-adaptation mechanism. That is, the bacteria respond quickly to changes in their environment and, on a slower time scale, adapt to these changes. Translated into run and tumble frequencies, improving the environment yields a decrease in tumble probabilities (signifying longer runs) with an eventual adaptation to return to a basal tumbling frequency. Such a mechanism implies that at least two time scales are involved: the rapid time scale of excitation and the slower time scale of adaptation. We shall see in this paper that the interplay of these two time scales can have important effects on the behavior of populations of bacteria near the maxima of the chemoattractant. Other time scales (or length scales, given that the swim speed of bacteria is roughly constant) also affect the chemotactic process. Three further scales of importance are the average periods of a run and of a tumble, and the physical length scale of the problem. In this work, we assume the sensory mechanism of the bacteria, through the excitation-adaptation process, affects only the probability of entering a tumble (the tumbling frequency), but that the time scale of tumbles are fixed. This assumption, which not entirely true biologically, is supported in realistic experimental settings [2].

When considering a large population of bacteria over long length scales, the macroscopic process is most often described mathematically using a Keller-Segel [9] reaction-diffusion model for $\rho(x,t)$, the density of bacteria. In its simplest form it reads

$$\rho_t = D\Delta\rho - \nabla\cdot(\chi(S)\rho\nabla S)$$

The first term on the right is a Fickian diffusion term arising from the unbiased random walk, whereas the second term introduces an advection speed proportional to the gradient of a chemoattractant $S(x)$, thus giving a bias in the mean displacement of the bacterial population. In this model, $\chi > 0$ is often reffered to as the chemotactic coefficient, and we have assumed that the chemoattractant concentration is given. These types of models have been shown to capture much of the important population-level behavior observed in bacteria [11]. An interesting class of Keller-Segel models arises when the chemoattractant itself is produced by the bacteria, which leads to spontaneous cluster formations [3, 10, 12].

At the organism level, simulations of the entire biochemical network of the chemotactic system have been undertaken at various levels of detail. In fact, the chemotactic mechanism of *Escherichia coli*, from the molecular sensing at the receptors on the bacterial surface to the flagellar motor drive, is one of the best understood cell-level biochemical processes. Bray et al. have created a detailed organism-level stochastic model for *E. coli* incorporating all of the known biological processes and experimentally-derived rate constants [5]. Simulated populations of these synthetic bacteria yield behavior that is comparable to real bacteria even down to predicting the behavior of specific mutant strains. Of course these fine-grained simulations are far more detailed and costly to com-

pute than Keller-Segel solutions.

We encountered the first motivation for this research in some of the simulation results of the Bray model [5]. In certain situations they observe a behavior for a population of bacteria in which the bacteria regularly overshoot the peak in chemoattractant concentration. This behavior occurs due to the sensing mechanism of the bacteria, which is sometimes unable to immediately respond to sharp changes in chemoattractant gradients. In populations of bacteria, the resulting density profiles have a volcano-like shape, with maximal bacterial densities occurring on a ring around the peak in chemoattractant concentration. This is what we mean by the *"volcano effect"*.

There is also some biological evidence supporting these stochastic results. As far back as 1973, Adler noted that bacteria would congregate some distance away from a nutrient source in capillary assays [1] . More recently, Mittal et al. have both experimental and modeling evidence of a maximal density being away from the highest concentration of chemoattractant in the case where bacteria are secreting their own chemoattractant in order to form clusters [10] .

A common question arising in these types of phenomena is how to coarse-grain from an organism-level model to a population-level model. Some methods follow a "gas-dynamics" approach and involve writing a Boltzmann equation for the bacterial density with a collision kernel accounting for the tumbling and reorientation [6]. Another approach considers including a simplified internal biochemical model explicitly as part of the state space. Recently, Erban and Othmer used such an approach and were able to derive a Keller-Segel equation modeling the behavior of the population. Their method involved writing a transport equation in state space and taking moments with respect to the bacteria's internal dynamical variables. Under certain assumptions about the scaling of time and space, the mean bacterial population was shown to obey Keller-Segel [7].

The Keller-Segel model does not have volcano-like behavior, and its steady solutions

$$\rho \sim exp\left[\frac{1}{D}\int^{S} \chi \, dS\right]$$

have maxima in bacterial concentration that coincide with the maxima of the chemical concentration. The aim of this work is to derive a continuum-level model, from a simple organism-level model, which can exhibit the "volcano effect" in the presence of rapid changes in the gradient of chemoattractant. Here, we propose two models which are able to capture this phenomenon, each derived from basic bacterial behavior and relying on two different aspects of the chemotaxis mechanism and response.

2. Formulation

In order to derive continuum-level equations from an organism-level model, we will follow a similar approach to Erban and Othmer [7]. This approach involves writing transport equations in the full state space (physical space,

velocity, and internal biochemical variables) and then taking moments over the internal variables. We shall use a simple 2-variable model describing the excitation-adaptation state of individual bacteria. The result are equations for the density and flux of the bacterial population and for the departures from the equilibrium values of the internal variables. These equations have to be supplemented by closures which express higher moments as a function of known quantities.

2.1. Transport equations

Letting the bacterial density be $p(x, v, z, t)$, a function of the spatial position $x \in \mathbb{R}^N$, velocity $v \in \mathbb{R}^N$, internal state variables $z \in \mathbb{R}^M$ (representing the concentrations of chemicals involved in the the chemotactic pathway), and time t, one assumes that the behavior of the internal state variables may be modeled by a system of ordinary differential equations

$$\frac{dz}{dt} = f(z, S).$$

At the most complex level, $f(z, S)$ is given by the full mass-action kinetics of the chemotactic pathway and may include thousands of variables as in [5]. $S(x)$ is the given external chemoattractant concentration. One then writes a transport equation for the evolution of the density p

$$\frac{\partial p}{\partial t} + \nabla_x \cdot vp + \nabla_z \cdot fp = Q(p, z)$$

where Q is a "collision kernel", or the term that incorporates changes in the velocity of the bacteria due to tumbling.

In order to simplify the problem and isolate different effects, in this paper we focus on the one-dimensional physical problem (bacteria on a line) and the simplest excitation-adaptation system with $z \in \mathbb{R}^2$. This is the case considered in [7], and then generalized to higher spatial dimensions in [8]. Assuming discrete velocities of $\pm s$ or 0 (for right-moving, left-moving or tumbling bacteria, respectively), one may consider three subpopulations of bacteria:

$$p^\sigma(x, z, t) = p(x, \sigma s, z, t), \qquad \sigma = +, -, 0.$$

This results in three transport equations:

$$\begin{aligned} \frac{\partial p^+}{\partial t} + s\frac{\partial p^+}{\partial x} + \nabla_z \cdot fp^+ &= Q^+(p^+, p^-, p^0, z) \\ \frac{\partial p^0}{\partial t} \qquad\qquad + \nabla_z \cdot fp^0 &= Q^0(p^+, p^-, p^0, z) \\ \frac{\partial p^-}{\partial t} - s\frac{\partial p^-}{\partial x} + \nabla_z \cdot fp^- &= Q^-(p^+, p^-, p^0, z) \end{aligned} \tag{1}$$

The terms Q^σ should now be seen as transition probabilities between states. In order to examine the behavior of the observable population of bacteria (internal

variables are not directly observable in most experimental settings), we define

$$n(x,t) = \int (p^+ + p^-)dz, \qquad m(x,t) = \int p^0 dz, \qquad j(x,t) = s\int (p^+ - p^-)dz,$$

where n is the density of swimming bacteria, m, that of tumbling bacteria, and j is the flux of bacteria at (x,t). The observable density is $n+m$. We also introduce higher moments of n, m, and j with respect to z as follows:

$$n^{i,k} = \int z_1^i z_2^k (p^+ + p^-)dz \qquad m^{i,k} = \int z_1^i z_2^k p^0 dz \qquad j^{i,k} = s\int z_1^i z_2^k (p^+ - p^-)dz$$

In order to derive evolution equations for these quantities, we take moments of the transport equations for a specific form of $f(z,S)$ and Q^σ in the following section.

2.2. Excitation-adaptation model

A simple model of the internal state of a bacterium may be described using two variables, denoted by y_1 and y_2 (we shall return to z briefly). The variable y_1 will vary on the time scale of the excitation, whereas y_2 will vary on a slower time scale of adaptation. An excitation-adaptation model may be written as:

$$\frac{dy_1}{dt} = \frac{g(S) - (y_1 + y_2)}{t_e}$$
$$\frac{dy_2}{dt} = \frac{g(S) - y_2}{t_a}$$

where $g(S)$ describes how the sensing mechanism of the bacterium transmits the external chemical concentration S to an internal biochemical signal. The function g should be monotonically increasing as a function of S for a biologically-relevant model. This model imposes that a bacterium introduced to a step-wise change in chemoattractant concentration first responds rapidly by adjusting y_1 to $g(S) - y_2$ and then more slowly adapts y_2 to the new value of $g(S)$ with y_1 relaxing to zero.

In *E. coli*, y_1 can be thought of as the concentration of the protein CheY, which modulates the tumbling frequency by biasing the flagellar motor. The variable y_2 may be associated with CheA, which is associated with the receptor dynamics and the sensing of the external environment [11]. We normalize the variables y_1 and y_2 about their equilibria by letting $z_1 = y_1$ and $z_2 = y_2 - g(S)$. This will allow us to take moments in z_1 and z_2 about 0. Noting that S depends implicitly on t through the motion of the bacteria, the internal dynamics are now written

$$\begin{aligned} \frac{dz_1}{dt} &= \frac{-z_1 - z_2}{t_e} \equiv f_1(z_1, z_2) \\ \frac{dz_2}{dt} &= -\frac{z_2}{t_a} - g'(S)\big(\nabla S \cdot v\big) \equiv f_2(z_1, z_2), \qquad v = \pm s, 0. \end{aligned} \tag{2}$$

Clearly, z_1 and z_2 tend towards 0 for a constant value of S. If ∇S is non-constant, the internal biochemistry of a running bacteria is *always* off-equilibrium and never fully adapts. It is this fact that drives chemotactic behavior: if the bacteria were able to adapt during a run, then chemotaxis would not be possible.

2.3. Transition probabilities

In order to derive simple flux equations for n, m, and j from the transport equations (1), a model for the transitions Q^σ between the three velocity states is needed. Here again we will assume a simple model. In the case that the times spent running or tumbling in a uniform environment are exponentially distributed, for which there is experimental evidence [2], then the probability of entering a tumble may be considered as λdt. It is also necessary that λ be dependent on z_1, the measure of the adaptation level of the bacteria. If $z_1 = 0$, the bacteria are fully-adapted to their environment and enter a tumble with a basal tumbling frequency, which we will call $2\lambda_0$ (the factor of 2 will facilitate a comparison of models later). Assuming a simple linear model, and since an elevated level of z_1 implies an improvement in the environment and therefore a decrease in tumbling frequency, we define:

$$\lambda(z_1) = 2\lambda_0 - 2bz_1$$

for some constant b. Mathematically, λ needs to be above 0 to make sense as a tumbling frequency. Using the steady-state solution for z_1, we impose the constraint on the maximum chemoattractant gradient:

$$\lambda_0 > bst_a max\{g_x\}. \tag{3}$$

From a biological perspective, this expression for λ could be thought of as the linearization of a more complicated relation for small z_1.

Assuming that the frequency of exiting a tumble be independent of the internal state (for which there is also support in [2]), and representing this also by a Poisson process with rate β_0 with the bacteria choosing equally between left and right directions, the forms for the Q quantities may be written:

$$\begin{aligned} Q^+ &= -(2\lambda_0 - 2bz_1)p^+ + \frac{\beta_0}{2}p^0 \\ Q^0 &= (2\lambda_0 - 2bz_1)\big(p^+ + p^-\big) - \beta_0 p^0 \\ Q^- &= -(2\lambda_0 - 2bz_1)p^- + \frac{\beta_0}{2}p^0 \end{aligned}$$

2.4. Simplified cases

There are simplified cases we will consider throughout this paper. First of all, one could have a system with very short excitation time. The limit $t_e = 0$ in (2), which we denote *fast excitation*, implies that $z_1 = -z_2$ and that

$$\frac{dz_1}{dt} = -\frac{z_1}{t_a} + g'(S)\big(\nabla S \cdot v\big), \qquad v = \pm s, 0.$$

A second simplification is the removal of a tumbling state. In this case $p^0 = 0$ which corresponds to the limit $\beta_0 \to \infty$. One should note that the tumbling state is not completely "passive", given that the internal excitation-adaptation dynamics (as a return to $z_j = 0$) is still operating during tumbling. Thus we have four possibilities: (i) fast-excitation and no tumbling, (ii) fast-excitation with tumbling, (iii) slow excitation and no tumbling, and (iv) slow excitation with tumbling.

3. Conservation laws for moments

In order to obtain the moment flux equations for the population, we take linear combinations of equations (1) with the forms for f and Q chosen, and with weights $\pm 1, \pm s, z_1$ or z_2, integrate over z and obtain the following

$$\begin{aligned}
n_t + j_x &= -2\lambda_0 n + 2bn^{1,0} + \beta_0 m \\
j_t + s^2 n_x &= -2\lambda_0 j + 2bj^{1,0} \\
m_t &= 2\lambda_0 n - 2bn^{1,0} - \beta_0 m \\
n_t^{1,0} + j_x^{1,0} &= -\left(2\lambda_0 + \frac{1}{t_e}\right) n^{1,0} + 2bn^{2,0} - \frac{1}{t_e} n^{0,1} + \beta_0 m^{1,0} \\
j_t^{1,0} + s^2 n_x^{1,0} &= -\left(2\lambda_0 + \frac{1}{t_e}\right) j^{1,0} + 2bj^{2,0} - \frac{1}{t_e} j^{0,1} \\
m_t^{1,0} &= 2\lambda_0 n^{1,0} - 2bn^{2,0} - \frac{1}{t_e} m^{0,1} - \left(\beta_0 + \frac{1}{t_e}\right) m^{1,0} \\
n_t^{0,1} + j_x^{0,1} &= -sg' S_x j - \left(2\lambda_0 + \frac{1}{t_a}\right) n^{0,1} + 2bn^{1,1} + \beta_0 m^{0,1} \\
j_t^{0,1} + s^2 n_x^{0,1} &= -s^2 g' S_x n - \left(2\lambda_0 + \frac{1}{t_a}\right) j^{0,1} + 2bj^{1,1} \\
m_t^{0,1} &= 2\lambda_0 n^{0,1} - 2bn^{1,1} - \left(\beta_0 + \frac{1}{t_a}\right) m^{0,1}
\end{aligned} \tag{4}$$

These moment flux equations are not closed, and closing them requires expressing the higher order moments $n^{2,0}, n^{1,1}, j^{2,0}$, and $j^{1,1}$ as functions of the lower order moments. Initially, we will take these higher order moments to be zero. We now nondimensionalize the full system (4) with

$$\begin{aligned}
\hat{x} &= \frac{x}{st_a}, & \hat{t} &= \frac{t}{t_a}, & \hat{n} &= \frac{n}{n_0}, & \hat{j} &= \frac{j}{sn_0} \\
\hat{n}^{0,1} &= \frac{n^{0,1}}{S_0 n_0}, & \hat{j}^{0,1} &= \frac{j^{0,1}}{sS_0 n_0}, & \hat{n}^{1,0} &= \frac{n^{1,0}}{S_0 n_0}, & \hat{j}^{1,0} &= \frac{j^{1,0}}{sS_0 n_0} \\
\hat{\lambda}_0 &= \lambda_0 t_a, & \hat{b} &= bS_0 t_a, & \hat{\beta}_0 &= \frac{\beta_0}{t_a}, & \hat{S} &= \frac{S}{S_0}
\end{aligned}$$

(We have let n_0 be the scale of the density n and S_0 be the scale of concentration of chemoattractant S.) In addition to the dimensionless $\hat{\lambda}_0, \hat{\beta}_0, \hat{b}$, we

have introduced the ratio of excitation to adaptation timescales $\tau = t_e/t_a < 1$, which may be quite small for biologically relevant scenarios. Dropping the hats for ease of notation and writing the equations in terms of total population of bacteria $\rho = n + m$, the resulting nondimensional, closed system is

$$\begin{aligned} \rho_t + j_x &= 0 \\ j_t + (\rho - m)_x &= -2\lambda_0 j + 2b j^{1,0} \\ m_t &= 2\lambda_0(\rho - m) - 2b(\rho^{1,0} - m^{1,0}) - \beta_0 m \end{aligned} \tag{5}$$

$$\begin{aligned} \rho_t^{1,0} + j_x^{1,0} &= -\tau^{-1}\rho^{1,0} - \tau^{-1}\rho^{0,1} \\ j_t^{1,0} + (\rho^{1,0} - m^{1,0})_x &= -\big(2\lambda_0 + \tau^{-1}\big) j^{1,0} - \tau^{-1} j^{0,1} \\ m_t^{1,0} &= 2\lambda_0(\rho^{1,0} - m^{1,0}) - \tau^{-1} m^{0,1} - \big(\beta_0 + \tau^{-1}\big) m^{1,0} \end{aligned} \tag{6}$$

$$\begin{aligned} \rho_t^{0,1} + j_x^{0,1} &= -g' S_x j - \rho^{0,1} \\ j_t^{0,1} + (\rho^{0,1} - m^{0,1})_x &= -g' S_x(\rho - m) - \big(2\lambda_0 + 1\big) j^{0,1} \\ m_t^{0,1} &= 2\lambda_0(\rho^{0,1} - m^{0,1}) - \big(\beta_0 + 1\big) m^{0,1} \end{aligned} \tag{7}$$

This is the model we shall consider for the remainder of the paper, with various simplifications to isolate certain effects. The subcases (i)-(iv) listed above can be obtained with simplifications of these equations. (i) fast-excitation and no tumbling: use the first two equations of (5), (7), set all m variables to zero and in (5) set $j^{1,0} = -j^{0,1}$, (ii) fast-excitation with tumbling: use (5), (7), and in (5) set $\rho^{1,0} = -\rho^{0,1}$, $j^{1,0} = -j^{0,1}$, $m^{1,0} = -m^{0,1}$ (iii) slow excitation and no tumbling: use the first two equations of (5)–(7), set all m variables to zero, (iv) slow excitation with tumbling: use the full model.

4. The Keller-Segel equation

In order to derive a Keller-Segel model from equations (5)–(7), the spatio-temporal scales of interest are important. The flux equations derived in section 3 were derived using the scales affecting individual bacteria: the temporal scales of the excitation-adaptation behavior of the internal states and the spatial scales implied by an average bacterial velocity, s. This corresponds to time scales on the order of milliseconds to seconds and spatial scales on the order of micrometers.

Keller-Segel-type models are used to model populations of bacteria on large spatial scales and long time scales. For such population densities of bacteria, relevant spatial scales are on the order of millimeters to centimeters and time scales of the motion of populations are on the order of hours to days. In our problem the observational scale is set by the fixed chemoattractant concentration $S(x)$. Clearly the important scale in the equations is the scale over which

the chemotactic gradient varies. Thus, one may define the spatial scale of interest as, for example,

$$L = \frac{\int_\Omega |S_{xx}| dx}{\sum_{x_j \in \Omega} |S_{xx}(x_j)|}$$

The numerator is the total variation of the S_x, and x_j are the point at which S_{xx} attains local extrema. Thus L is the smallest distance over which the changes in S_x may have occured. If we non-dimensionalize the flux equations with spatial scale L instead of st_a (the length scale for individual bacterial runs), this is equivalent to introducing $\tilde{x} = \epsilon x$ where $\epsilon = \frac{st_a}{L}$. The dimensionless quantity ϵ is the bacterial swimming equivalent to the *Knudsen number* in molecular considerations of fluid mechanics. First, we assume that $\epsilon \ll 1$, which is true for smooth gradients, and where we expect Keller-Segel models apply. The fundamental balance $\rho_t + j_x = 0$ must be satisfied by any chosen scaling. By definition, $\rho, m = O(1)$ and thus a consistent choice is $j = O(\epsilon)$ and $t = O(\epsilon^2)$. This is the scaling we use for the remainder of this section, and results in time scales of $L^2/s^2 t_a$.

This scaling of time and space also implies the rescaling of other quantities:

$$j^{0,1} \to \epsilon j^{0,1}, \qquad j^{1,0} \to \epsilon j^{1,0}, \qquad \rho^{0,1} \to \epsilon^2 \rho^{0,1}, \qquad \rho^{1,0} \to \epsilon^2 \rho^{1,0},$$
$$m^{0,1} \to \epsilon^2 m^{0,1}, \qquad m^{1,0} \to \epsilon^2 m^{1,0}.$$

Regarding ϵ and τ as independent parameters, we obtain from (6), to leading order in ϵ,

$$\begin{aligned} \rho^{1,0} &= -\rho^{0,1} \\ m^{1,0} &= -\frac{2\tau\lambda_0}{\tau\beta_0 + 1}\rho^{0,1} - \frac{1}{\tau\beta_0 + 1} m^{0,1} \\ j^{1,0} &= -\frac{1}{2\tau\lambda_0 + 1} j^{0,1} \end{aligned}$$

Therefore, the closed leading-order equations governing this scaling, from (5) and (7) become:

$$\begin{aligned} \rho_t + j_x &= 0 \\ \frac{\beta_0}{2\lambda_0 + \beta_0}\rho_x &= -2\lambda_0 j + 2b j^{1,0} \\ 0 &= \big(2\lambda_0 + 1\big)(2\tau\lambda_0 + 1) j^{1,0} - g' S_x \frac{\beta_0}{2\lambda_0 + \beta_0}\rho \end{aligned}$$

This results in the Keller-Segel model

$$\rho_t = D\rho_{xx} - \partial_x(\chi \rho S_x)$$

with coefficients for diffusion and a chemotactic velocity given by

$$D = \frac{\beta_0}{2\lambda_0(2\lambda_0 + \beta_0)}$$
$$\chi(S) = \frac{b\beta_0 g'(S)}{\lambda_0(2\tau\lambda_0 + 1)(2\lambda_0 + 1)(2\lambda_0 + \beta_0)}$$

Hence, this formal calculation to leading order in appropriate scaling arguments results in the Keller-Segel model at a population level.

5. Models for a volcano

As we have seen, the Keller-Segel model attains steady-state extrema at the corresponding extrema of the chemoattractant concentration. There is evidence that this is not always the case, in both biological experiments and stochastic models. Thus, we would like to explore whether the simple excitation-adaptation model is capable of "volcanic" behavior in stochastic simulations of large numbers of individual bacteria, and, if so, we would like to find an appropriate population-level model which reproduces this volcano effect.

Biologically, the cause of a volcano effect is that the bacterium cannot sense rapid changes in its environment quickly enough. The result is that as a bacterium crosses a sharp peak in chemoattractant concentration and its environment starts deteriorating suddenly, the bacteria continue to run in the same direction for a short period of time before sensing the deterioration. Once it senses that its direction is no longer optimal, it reorients with higher frequency, and will again have a similar overshoot if it crosses back over the peak in concentration of chemoattractant in any subsequent runs.

It seems clear that the simple excitation-adaptation model with the transition model proposed would give rise to such overshoots: consider the simplest case of $t_e = 0$ and no tumbling state. A bacterium in a long run towards a peak in concentration will have a $\lambda < \lambda_0$, and this will remain true for a finite amount of time $O(t_a)$ after it crosses the peak. Thus, over a distance $O(st_a)$, it will have a probability of turning around which is lower than λ_0, as if it "believed" the environment were still improving. This can be observed in stochastic simulations of bacteria. In terms of bacterial density, however, there is a subtlety. Even with overshoots, the maximum *density* would occur at the peak in concentration, for that is the most likely place for the bacterium to be, even if it is just passing through. Now consider introducing back the tumbling state: since tumbling occurs most often slightly away from the peak in concentration by the previous argument, a finite time spent tumbling make bacteria more likely to be *observed* away from the peak. As we shall see this will be one way to obtain a volcano in a continuum model.

In fact, in the models considered in this paper, there are two factors that might give rise to a volcano effect: the overshoot described above related to the finite time a bacterium takes to adapt to a worsening environment, and the effect of finite excitation times. The differences between the two factors are real,

but subtle. Of course, both factors involve small spatial scales and the fact that the bacteria take some time to sense and adapt to the external environment. As we have argued in the previous paragraph, in the first scenario, a tumbling state is required. In the second, we shall see that a tumbling state is not required. Later in the paper we will discuss how these two factors interact when both are present. As it turns out, the two factors combined do not simply result in a stronger volcano effect.

The second possible cause for a volcano, the case where there is a non-zero excitation time t_e, means that the sensing mechanism has a "delay": it takes a short period of time for the bacteria to become aware of its surroundings. With such a delay, it is possible that the bacteria will not congregate at the peak concentration, but instead on either side of it. The reason for this is that the bacterium can confuse improving and deteriorating environments since it is effectively sensing its environment from a short time before. Suppose a bacterium has crossed the peak and is within a region of decreasing concentration: it will eventually sense this and turn around. As it now climbs the gradient it will be for a while mistaken (since its *excitation* time is finite) and therefore more likely to tumble sooner than it should. This may repeat a few times until it makes a longer run and crosses the peak again. The net result is that it will therefore spend a finite time on each side of the peak in concentration in a seemingly "confused" zig-zag.

In order to obtain a volcano effect in numerical simulations of individual bacteria, as Bray et al. [5] have done, as well as in experiments with live bacteria, one must have an abrupt change in chemoattractant gradients. Thus, we can no longer assume $\epsilon \ll 1$ and we must return to the full flux equations (4). In order to explore this further, we first consider the case where S has a single sharp peak centered at $x = 0$. In controlled chemotaxis experiments the concentration profile of $S(x)$ is usually chosen such that $g'S_x$ is constant, or rather that $g(S)$ is linear, so we shall approximate $g'S_x$ near a peak at $x = 0$ as:

$$g'S_x = \begin{cases} a, & x < 0 \\ -a, & x > 0 \end{cases} \tag{8}$$

In the rest of this section, we will use this form for $g'S_x$, reducing the system to having constant coefficients, together with appropriate continuity conditions at $x = 0$. Since $g(S)$ must be monotonic in S to be biologically relevant, a sharp peak in $S(x)$ will correspond to a sharp peak in $g(S)$ and vice-versa. We shall consider two limiting cases: fast-excitation with tumbling and slow excitation and no tumbling (cases (ii) and (iii) introduced before). It is worth nothing that this assumption implies $L = 0$ or $\epsilon = \infty$. In practice this is of course not possible (one cannot maintain such a sharp S which would itself diffuse), but is a useful approximation. Later in the paper we shall consider numerical simulations with sharp, yet not discontinuous, changes in the gradient.

5.1. Tumbling and fast excitation behavior

We return to the model (4), assuming that the excitation time $t_e = 0$. As was pointed out above, the 9 equations reduce to 6 equations. When seeking steady-state solutions, the system can be reduced to 3 equations since $j = 0$ and since $\rho, \rho^{0,1}, m$, and $m^{0,1}$ may be expressed as functions of n, and $n^{0,1}$. This linear system is

$$\begin{pmatrix} n \\ j^{0,1} \\ n^{0,1} \end{pmatrix}_x = - \begin{pmatrix} 0 & 2b & 0 \\ 0 & 0 & \frac{2\lambda_0+\beta_0+1}{\beta_0+1} \\ g'S_x & 2\lambda_0+1 & 0 \end{pmatrix} \begin{pmatrix} n \\ j^{0,1} \\ n^{0,1} \end{pmatrix} \tag{9}$$

Since $g'S_x$ is symmetric about $x = 0$, we shall seek solutions to (9) for which n and $n^{0,1}$ are symmetric about $x = 0$ and $j^{0,1}$ is antisymmetric. This allows us to consider the domain of x to be $\mathbb{R}^+$ and implies that $j^{0,1} = 0$ at $x = 0$ (or, equivalently, $n_x = 0$ at $x = 0$). The problem may then be posed as:

$$\begin{aligned} &\mathbf{n}_x = A\mathbf{n}, x \in \mathbb{R}^+ \\ &\mathbf{n}(0) = (N, 0, N^{0,1})^T \\ &\mathbf{n}(x) \to \mathbf{0} \text{ as } x \to \infty \end{aligned} \tag{10}$$

for N and $N^{0,1}$ real-valued constants. Note that $n^{0,1}$ need not have a continuous derivative at $x = 0$ since $g(S)$ does not. The solutions depend, of course, on the eigenvalues of matrix A. One can show that there is one positive real-valued eigenvalue and hence there are either two negative real-valued or two complex conjugate eigenvalues. To avoid biologically unrealistic solutions with negative densities, we avoid complex eigenvalues by imposing the restriction

$$g_x \leq \sqrt{\frac{(2\lambda_0+1)^3}{27b^2}} \tag{11}$$

We must also impose that the solution lies in the eigenspace of the two negative real eigenvalues so that it does not grow exponentially. This fixes a relation between N and $N^{0,1}$, and this relation implies that if $N > 0$, $N^{0,1}$ is negative.

The population density ρ can be recovered from solutions with

$$\rho = n + m = n + \frac{2\lambda_0}{\beta_0} n + \frac{2b}{\beta_0} n^{0,1}.$$

First we consider the case of no tumbling, which can be obtained by taking $\beta_0 \to \infty$. Then $\rho = n$ and therefore, at $x = 0$: $\rho = N > 0$, $\rho_x = 0$ and $\rho_{xx} = 2bn^{0,1} = 2bN^{0,1} < 0$. These imply a local maxima in ρ at $x = 0$, and no volcano effect. Therefore, without tumbling and with $t_e = 0$, a volcano-like population density cannot occur.

However, with the tumbling population the situation changes since $n_x^{0,1} > 0$ as $x \to 0^+$. (To see this, consider the problem on the whole real line which shows there must be a jump in $n_x^{0,1}$ at $x = 0$ from the $-g'S_x n$ term.) Then $\rho_x = \frac{2b}{\beta_0} n_x^{0,1} > 0$ as $x \to 0^+$ and, by symmetry, ρ has a local minimum at $x = 0$

in the form of a corner. Since we also know the ρ must decay to 0 as $x \to \pm\infty$, there must be a maximum value for ρ at some finite value of x away from 0, resulting in a volcano.

This simple system also allows for an estimate for the height and width of a volcano. Approximating ρ about $x = 0$ as $\rho \approx c_0 + c_1|x| + \frac{1}{2}c_2x^2$ for $c_0 > 0$, $c_1 > 0$ and $c_2 < 0$ constants. With some algebra, this approximation allows for one to solve for c_1 and c_2 in terms of the parameters of the system (λ_0, β_0, b, and a). Then, calculating the approximate height and width of the volcano is simple, giving a height $c_1^2/2c_2$ and width $2c_1/c_2$. Figure 1(a) shows the exact solution of the linear system together with this approximation.

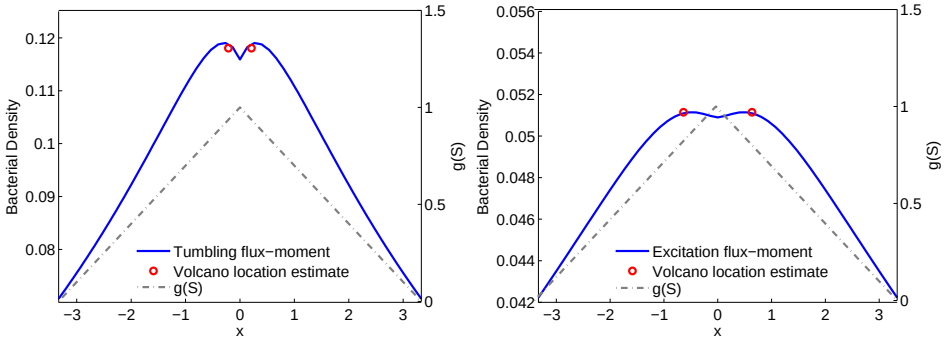

(a) Tumbling model with $\beta_0 = 1$.

(b) Excitation model with $\tau = 0.5$.

Figure 1: Moment flux solution and volcano size estimates for both flux models with $\lambda_0 = 1, b = 1, a = 0.3$ and $g(S) = 1 - a|x|$.

5.2. Slow excitation without tumbling

We turn to the case where the bacteria sense changes in their environment more gradually with $t_e \neq 0$, but that there is also no tumbling state so that the transitions are now directly between right- and left-moving bacteria (case (iii) mentioned above). We may restrict ourselves to the first two equations of each set (5)–(7) with m and its moments set to zero. (An *ab initio* derivation of these flux equations for a model with no tumbling requires that $\lambda(z_1) = \lambda_0 - bz_1$, without the factors of two, to compensate for bacteria which now cannot return to a run in the same direction after tumbling.) Again, we are interested in steady-state solutions and $j(x)$ will be 0, and we restrict ourselves to the specific case where $g(S)$ takes the form (8). The result is the following system for $x \in \mathbb{R}^+$

$$\begin{pmatrix} n \\ j^{0,1} \\ n^{0,1} \\ j^{1,0} \\ n^{1,0} \end{pmatrix}_x = - \begin{pmatrix} 0 & 0 & 0 & -2b & 0 \\ 0 & 0 & 1 & 0 & 0 \\ -a & 2\lambda_0 + 1 & 0 & 0 & 0 \\ 0 & 0 & \tau^{-1} & 0 & \tau^{-1} \\ 0 & \tau^{-1} & 0 & 2\lambda_0 + \tau^{-1} & 0 \end{pmatrix} \begin{pmatrix} n \\ j^{0,1} \\ n^{0,1} \\ j^{1,0} \\ n^{1,0} \end{pmatrix}$$

Assuming $\tau \ll 1$, consider the following expansions in τ:

$$\begin{aligned} n &= \bar{n} + \tau\tilde{n} + O(\tau^2) \\ n^{i,k} &= \bar{n}^{\,i,k} + \tau\tilde{n}^{\,i,k} + O(\tau^2) \\ j^{\,i,k} &= \bar{j}^{\,i,k} + \tau\tilde{j}^{\,i,k} + O(\tau^2) \end{aligned}$$

The lowest order equations are

$$\begin{aligned} O(\tau^{-1}): \qquad \bar{n}^{\,1,0} &= -\bar{n}^{\,0,1} \\ \bar{j}^{\,1,0} &= -\bar{j}^{\,0,1} \end{aligned}$$

and the leading order corrections are

$$O(1): \qquad \bar{n}_x = -2b\bar{j}^{\,0,1} \tag{12}$$

$$\bar{j}_x^{\,0,1} = -\bar{n}^{\,0,1} \tag{13}$$

$$\bar{n}_x^{\,0,1} = -g'S_x\bar{n} - \Big(2\lambda_0 + 1\Big)\bar{j}^{\,0,1} \tag{14}$$

$$\bar{j}_x^{\,1,0} = -\tilde{n}^{\,1,0} - \tilde{n}^{\,0,1} \tag{15}$$

$$\bar{n}_x^{\,1,0} = 2\lambda_0\bar{j}^{\,0,1} - \tilde{j}^{\,1,0} - \tilde{j}^{\,0,1} \tag{16}$$

Equations (12) through (14) are of the same form as (9) and not coupled with equations (15) and (16). The system (12)–(14) has no volcano for n alone, just as in in section 5.1 (it was the $n^{0,1}$ term in m which caused the volcano in the previous case but now $m = 0$). Hence, at $O(1)$, there is no volcano-like behavior. Equations (15) and (16) allow us to write:

$$\begin{aligned} \bar{n}^{\,0,1} + \tilde{n}^{\,1,0} + \tilde{n}^{\,0,1} &= 0 \\ g'S_x\bar{n} + \bar{j}^{\,0,1} + \tilde{j}^{\,1,0} + \tilde{j}^{\,0,1} &= 0 \end{aligned}$$

At order τ, the equations for $\tilde{n}, \tilde{j}^{\,0,1}$, and $\tilde{n}^{\,0,1}$ are:

$$\begin{aligned} O(\tau): \qquad \tilde{n}_x &= -2bg'S_x\bar{n} - 2b\bar{j}^{\,0,1} - 2b\tilde{j}^{\,0,1} \\ \tilde{j}_x^{\,0,1} &= -\tilde{n}^{\,0,1} \\ \tilde{n}_x^{\,0,1} &= -g'S_x\tilde{n} - \Big(2\lambda_0 + 1\Big)\tilde{j}^{\,0,1} \end{aligned} \tag{17}$$

Equations (17) are again solvable and a closed system because $\bar{n}$ and $\bar{j}^{\,0,1}$ can be found from the order 1 equations. The equation for $\tilde{n}$ implies that it must have a jump in slope at $x = 0$ because of the $g'S_x\bar{n}$ term. This jump gives $\tilde{n}$ a volcano-like shape near $x = 0$.

Since we are interested in the quantity $n = \bar{n} + \tau\tilde{n}$, we may conclude that even without the tumbling state (m quantities), a volcano should be present with a non-zero excitation time due to this jump in slope of $\tilde{n}$ at $x = 0$. This

volcano effect will be of order τ since it is the result of the $\tilde{n}$ dynamics, so it should be a weak volcano in comparison to the one observed with the tumbling state. This is illustrated in figure 1. Additionally, an estimate of the height and width of the volcano is again possible, but this time we take $\rho = n = \bar{n} + \tau\tilde{n} \approx c_0 + \tau c_1|x| + \frac{1}{2}c_2x^2$, where we have ignored terms of $O(\tau x^2)$. The c_1 term now comes from the behavior of $\tilde{n}$. Again, using (12)–(14), we can estimate the values of c_1 and c_2 and therefore the height and width of the volcano. Figure 1(b) shows the results of this estimation, together with the solution of the linear system. Although we use a fairly large value of τ for emphasis, note that the volcano should exist for all values fixed values of $\tau > 0$.

6. Numerical solutions and comparisons

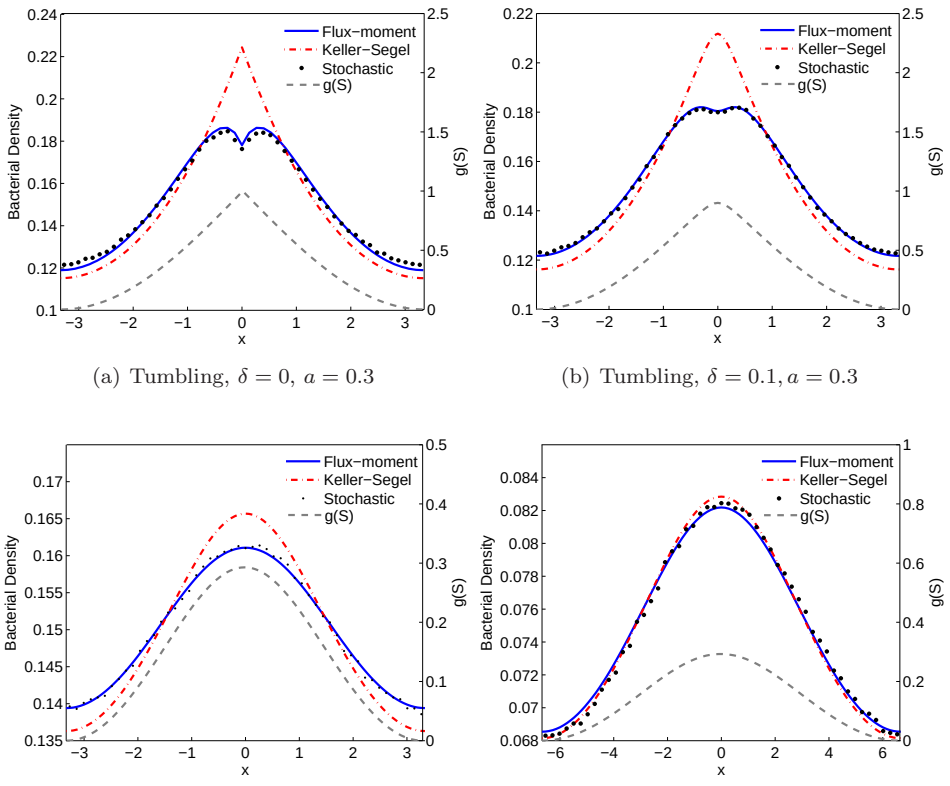

(a) Tumbling, $\delta = 0$, $a = 0.3$

(b) Tumbling, $\delta = 0.1, a = 0.3$

(c) Tumbling, $\delta = 1, a = 0.3$

(d) Tumbling, $\delta = 1, a = 0.15$

Figure 2: Tumbling moment flux model with $\lambda_0 = 1, b = 1, \beta_0 = 1$.

Continuum-level models, like the Keller-Segel equations and the flux model (5)–(7), describe the average behavior of a population of many bacteria governed

by stochastic models. Since they are only approximations, we now compare the continuum model and stochastic many-particle computations to verify whether the stochastic behavior is well-modeled by the continuum model. Additionally, we have only shown that volcano-like behavior occurs if $g'S_x$ is piece-wise constant. Here, we show numerical evidence for volcanos in the case that $g'S_x$ takes on different forms, and that the many-particle stochastic computations also yield volcanos. In our flux model computations, simple fourth-order Runge-Kutta schemes in time with finite differences in space are used. Keller-Segel solutions are found analytically.

The stochastic results are for large populations, making the density relatively smooth. A population of 4 million bacteria is simulated in each computation. For each bacterium, its velocity, internal state variables, and spatial position are computed deterministically at every time step of size $\Delta t \ll \lambda^{-1}$. The internal variables are evolved with equations (2). After each timestep the bacteria are randomly assigned to change their state (running or tumbling) according to their probability of tumbling (or turning if there is no tumbling in the model), $\lambda \Delta t$.

We restrict our comparisons to steady-state behavior, and, for the many-particle computations, we compute the densities when we believe statistical steady state is reached. Additionally, in all computations, we use the two-parameter (a, δ) periodic chemoattractant concentration function

$$g(S) = 1 - \frac{\sqrt{\frac{1}{2} + \delta^2 - \frac{1}{2}\cos(\pi x a)}}{\sqrt{1+\delta^2}}.$$

The parameters δ and a set the length scale and the maximum slope of the chemoattractant concentration. It is useful to be able to set these two quantities independently since both quantities enter in approximations we have made, and we must ensure that the two conditions 3 and 11 are satisfied. Thus

$$L \sim \frac{\delta}{a\sqrt{1+\delta^2}}, \qquad max\ g_x \sim \frac{a}{1+\delta^2}.$$

6.1. Steady-state solutions

Figures 2 (for fast excitation with tumbling) and 3 (for slow excitation and no tumbling) show the results in both smooth and non-smooth chemoattactrant concentrations. As the length scale of the problem increases (from top left to bottom right) we expect the stochastic model to result in the highest concentration of bacteria accumulating at the highest concentration of S (or, equivalently, a peak in $g(S)$ since $g(S)$ is monotonic in S) and expect Keller-Segel to agree well. In all cases, the moment flux model captures the behavior more accurately. In the case of sharp changes in the gradient of $S(x)$ the moment flux model is far more accurate and agrees with the stochastic computations that show a distinct volcano. In the smoother cases, Keller-Segel overestimates the chemotactic response of the bacteria, resulting in a higher peak in bacterial

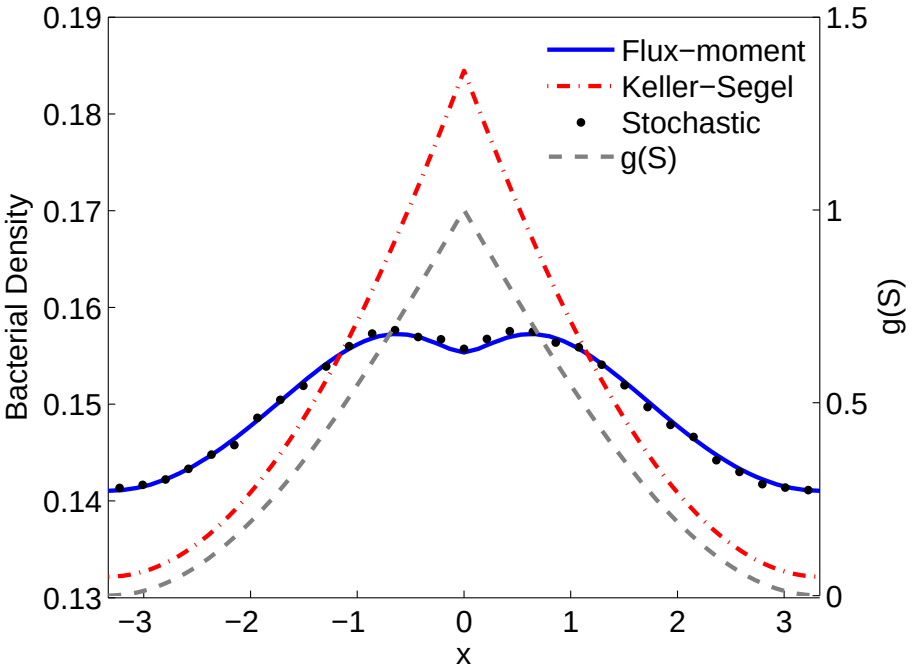

(a) $\delta = 0, a = 0.3$

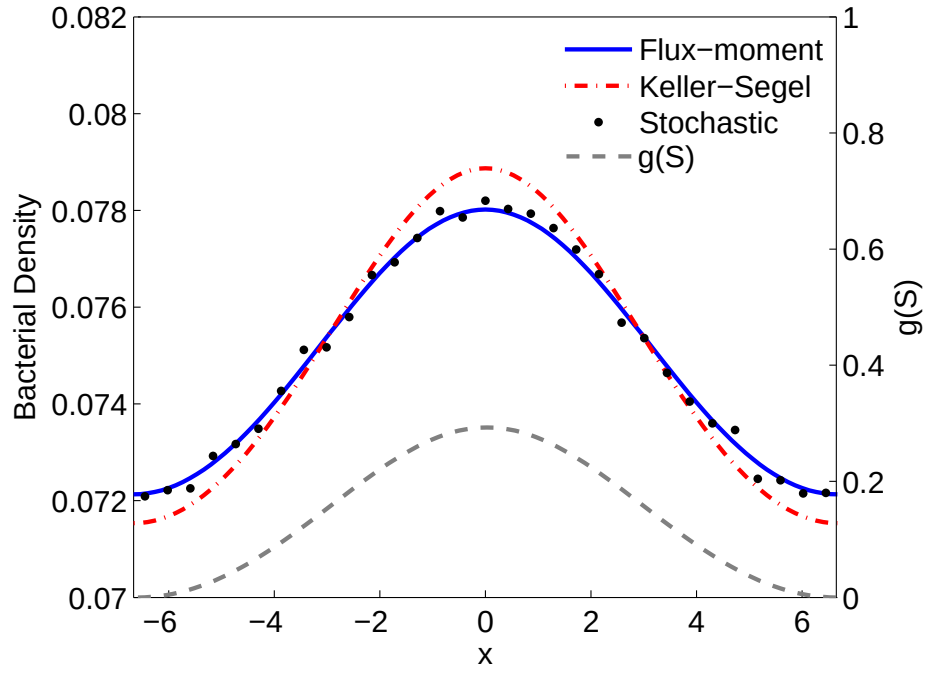

(b) $\delta = 1, a = 0.15$

Figure 3: Excitation moment flux model with $\lambda_0 = 1, b = 1, \tau = 0.5$.

density. Using Fourier expansion, one can quantify exactly by how much the Keller-Segel model overestimates the effects of chemotaxis over the moment flux model (see Appendix A).

In order to further understand the behavioral differences between the two models and why they exhibit the volcano effect, it is helpful to consider certain moments with respect to z_1 (which is the variable that modulates the tumbling frequency) of the right-moving and left-moving bacteria, i.e.

$$n^{1,0+} = \int z_1 p^+ dz_1 = \frac{1}{2}(n^{1,0} + j^{1,0}), \qquad n^{1,0-} = \int z_1 p^- dz_1 = \frac{1}{2}(n^{1,0} - j^{1,0})$$

These quantities give the mean of z_1, which is a measure of the level of excitation of right- and left-going bacteria at position x. Thus, we would expect $n^{1,0+}$ to have the same sign as the gradient of S and $n^{1,0-}$ to have the opposite. Another quantity, $sgn(S_x)bj^{1,0}$, can be interpreted as the difference in mean run lengths at a given point x between bacteria moving up a gradient and bacteria moving down a gradient. If the bacteria are chemotaxing correctly, it would be expected for them to have longer run lengths going up a gradient of the chemoattractant than down and therefore $sgn(S_x)bj^{1,0} > 0$. In the case of tumbling-only bacteria, we find that this is the case (see figure 4(a)), however, there is a region after the bacteria cross the peak of the gradient (see figure 4(b)) where they have the opposite sign of $n^{1,0+}, n^{1,0-}$ than expected. This means there are bacteria going in the wrong direction and are confused in believing that the environment is improving, and therefore have a low tumbling rate. Thus there is a lag time before their turning rate adjusts to the deteriorating environment and rises above the basal rate λ_0. Consequently, bacteria swim back and forth over the maximum and the volcano arises from them spending time tumbling away from the maximum.

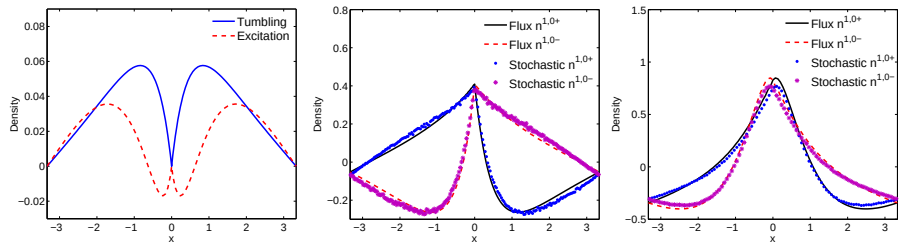

(a) Plot for $sgn(S_x)bj^{1,0}$. (b) $n^{1,0\pm}$, tumbling model. (c) $n^{1,0\pm}$, excitation model.

Figure 4: Comparison of tumbling and excitation models in terms of $sgn(S_x)bj^{1,0}$ and $n^{1,0+}$ and $n^{1,0-}$ with $\lambda_0 = 1, b = 1, \beta_0 = 1, \tau = 0.5$ and $\delta = 0$.

In the case of bacteria with a finite excitation time, $sgn(S_x)bj^{1,0} < 0$ for a region near the maxima, shown in figure 4(a). This means that for these bacteria, the runs are longer in the downgradient direction! That is, bacteria

will tend to zig-zag beside maximum concentration. In figure 4(c), not only there is a region where $n^{1,0+}, n^{1,0-}$ has the opposite sign than expected, but in fact, the *maximum* of these quantities lie in the wrong region. Just like in the tumbling case, this indicates that there are a significant number of bacteria running in the wrong direction in this region and that bacteria will spend a finite time on each side of the gradient seemingly "confused".

One can thus form a picture of the two effects. In the tumbling-only case, the volcano is generated by a delay in the adaptation dynamics that yield the "cartoon" of bacteria crossing the maximun back-and-forth and spending most of their time tumbling away from the peak of S. In the finite excitation time bacteria, the delay in excitation creates a situation in which there are a finite amount of direction reversals on either side of the peak of S that delay the bacteria there. In some sense, the finite excitation time has "created" a ghost of the tumble dynamics on their own on either side of the peak.

6.2. Time-evolution of bacterial densities

One may also compare the moment flux model to stochastic results for a bacterial density as it evolves from unstable initial data toward a steady-state. This also serves to illustrate the difference in behavior of the volcano effect due to tumbling as compared to a finite excitation time. In the case of tumbling, the bacterial population spreads towards the maximal concentration and a volcano effect begins to develop around the peak in $g(S)$ once the population reaches that location. This is shown in figure 5. In the case of excitation, a more complex transient behavior occurs, as seen in figure 6. One sees unstable peaks in bacterial density which are not always localized around the peak in $g(S)$. This behavior occurs due to this "zig-zag" confused behavior we have described earlier: the population's delayed sensing mechanism causes the bacteria to sense peaks and troughs in $g(S)$ at the wrong spatial coordinates. As the density evolves, it slowly averages out some of this incorrect sensing, but only where $g(S)$ is smooth, as it cannot correctly resolve the sharp change in the gradient of $g(S)$ at the peak. Additionally, in both models it is clear that this moment flux model is correctly modeling the average behavior of the stochastic model.

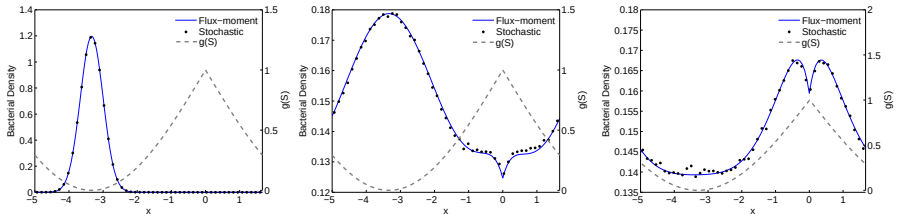

(a) Tumbling, $t = 0$. (b) Tumbling, $t = 12.5$. (c) Tumbling, $t = 21$.

Figure 5: Time evolution of a bacterial population with a tumbling state.

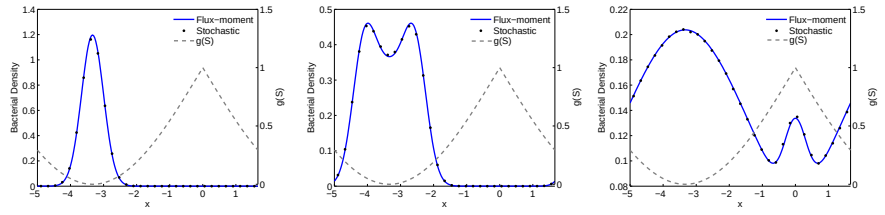

(a) Excitation, $t = 0$. (b) Excitation, $t = 0.8$. (c) Excitation, $t = 3.3$.

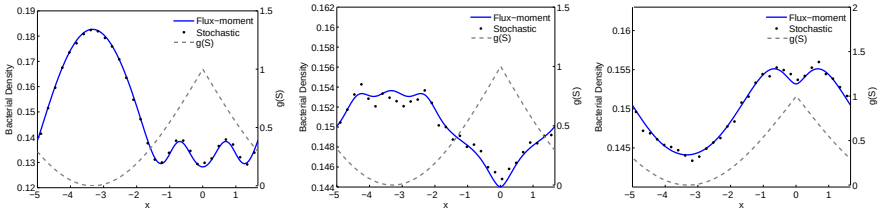

(d) Excitation, $t = 4.2$. (e) Excitation, $t = 5.8$. (f) Excitation, $t = 8.3$.

Figure 6: Time evolution of a bacterial population with a non-zero excitation time.

7. Other closures for the moment flux model

Other closures (other than setting higher moments to zero) for this system have been proposed in the work of Erban and Othmer [7]. The reason for considering other closures is to model the cases where g_x may be large and therefore moments with respect to z_j^2 may not be small compared with moments with respect to z_j. Erban and Othmer worked with a fast-adaptation model, in which one can propose the assumption that $z_2 \approx \mp g' S_x$ (in nondimensional form) which reduces the higher-order moments in z_2 to lower-order moments. There are two choices: either to assume that $z_2^2 \approx \mp g' S_x z_2$ or $z_2^2 \approx (g' S_x)^2$. Such closures might result in the better agreement with the stochastic results for large gradients, but *only* in the cases that they consider where the gradient is of one sign. This type of closure is assuming the bacteria are close to adapted to their environment which is precisely the opposite of what happens when a chemoattractant density has sharp changes in gradients and volcano behavior is observed. The less accurate agreement of this type of a closure (compared to the original closure) in the volcano setting is shown for both tumbling and excitation models in figure 7. In order to get a better closure for the model, one idea is to approximate z_2 with the type of closure described only for bacteria *climbing* a gradient. Bacteria descending a gradient should probably remain with the zero closure we have assumed throughout. One possibility is therefore that $m^{0,2} = 0$ and

$$n^{0,2} = \int z_2^2 (n^+ + n^-) \equiv \begin{cases} \int z_2^2 n^+ \approx -g_x \int z_2 n^+ = -\frac{1}{2} g_x (n^{0,1} + j^{0,1}), & g_x > 0 \\ \int z_2^2 n^- \approx g_x \int z_2 n^- = \frac{1}{2} g_x (n^{0,1} - j^{0,1}), & g_x < 0 \end{cases}$$

which can be rewritten

$$n^{0,2} \equiv -\frac{1}{2}|g_x|n^{0,1} - \frac{1}{2}g_x j^{0,1}.$$

Similarly,

$$j^{0,2} \equiv -\frac{1}{2}g_x n^{0,1} - \frac{1}{2}|g_x|j^{0,1}.$$

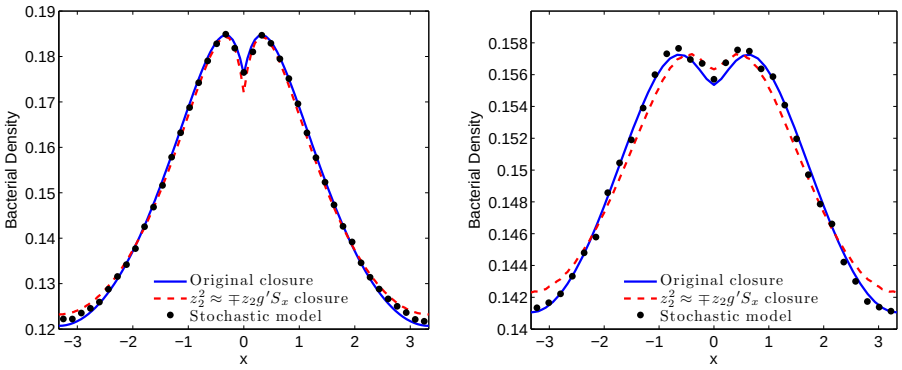

(a) Tumbling model, $\beta_0 = 1$.

(b) Excitation model, $\tau = 0.5$.

Figure 7: Original closure of moment flux model (taking higher order moments to be 0) as compared to the closure using $z_2^2 \approx \mp z_2 g' S_x$ and stochastic model with $\lambda_0 = 1, b = 1$ and $\delta = 0$.

8. Discussion

We have shown two effects which result in volcano-like steady state bacterial densities for abrupt changes in the environment. It is important to note that without either excitation time or a tumbling phase, regardless of what closure is chosen for the moment flux equations, it is not possible to obtain a volcano in the bacterial density. The idea is that the bacteria tend to spend more time on either side of a sharp change in chemoattractant gradient either because of a higher tumbling frequency in this region, or because of a delayed ability to sense its current environment.

While these are two mathematically different processes, biologically, the more relevant process appears to be the tumbling state. However, since clearly both an excitation phase and adaptation phase must be present in real bacteria, it is helpful to consider the full model with both tumbling and excitation phases. As it turns out, these two behaviors that cause a volcano do not create an all-around larger volcano when combined. The addition of a finite excitation time smoothens the tumbling-only solution: it decreases the height of the volcano while increasing the width slightly. An example of this is shown in figure 8.

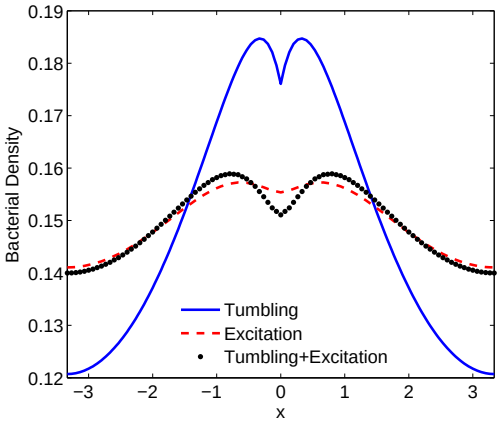

Figure 8: Comparison of tumbling alone, excitation alone, and tumbling and excitation moment flux models with $\lambda_0 = 1, b = 1, \beta_0 = 1, \tau = 0.5$ and $\delta = 0$ The height of the volcano for the combined model is approximately 10% smaller than the volcano of tumbling model.

One important mathematical question is one of positivity of ρ in the solutions: we have imposed some reasonable conditions on the maximum of g_x and, with that, have not encountered any problems. Thus, we believe that as modeling equations the system we propose is appropriate.

9. Conclusions and further work

One of the fundamental reasons for mathematical modeling in biology is to show that, whilst a biological problem may have thousands of parameters, the generic behavior may depend on a far fewer number. While our model has made some simple assumptions to approximate the biology involved, one could include a more complex biological description if desired, and the dynamics would reduce to the same type of overall system as long as it is governed by excitation-adaptation dynamics.

There are several areas which merit further work: first, one would like to extend this model to higher dimensions (chemotaxis is a 2- or 3-dimensional phenomena in most experimental settings), and to compare the model against actual experiments: either those mentioned above which motivated this work, or to new, more controlled experiments now that we have some understanding on what to expect and the scalings involved.

10. Acknowledgements

This research was funded by the U.S. Department of Energy Genomics: GTL and SciDAC Programs (DE-FG02-04ER25627).

Appendix A. Fourier expansions of moment flux solutions

One may use Fourier expansions to represent the densities n and m and their associated fluxes and moments for periodic chemoattractant concentrations. We consider here the simple form for $g'S_x$, namely $g(S) = A(1+\cos(\pi x/L))$ so that $g'S_x = -\frac{A\pi}{L}\sin(\pi x/L)$, to examine the steady-state solution of the tumbling flux equations (9). Now we use a Fourier expansion for $j^{0,1}$ and $g'S_x n$ by letting

$$
\begin{aligned}
j^{0,1} &= \sum_{k=1}^{\infty} a_k sin\left(\frac{k\pi x}{L}\right) \\
g'S_x n &= \sum_{k=1}^{\infty} b_k sin\left(\frac{k\pi x}{L}\right) \\
n &= \sum_{k=0}^{\infty} c_k cos(\frac{k\pi x}{L})
\end{aligned}
$$

Using equation (9) we obtain the following recursion relation for c_k

$$
\begin{aligned}
c_1 &= \frac{AbB}{\frac{\pi^2}{L^2} + (2\lambda_0 + 1)B}(2c_0 - c_2) \\
kc_k &= \frac{AbB}{\frac{k^2\pi^2}{L^2} + (2\lambda_0 + 1)B}(c_{k-1} - c_{k+1}) \quad \text{for } k \geq 2
\end{aligned}
\tag{A.1}
$$

where c_0 may be any constant and is proportional to the total population and $B = \frac{2\lambda_0+\beta_0+1}{\beta_0+1}$. (Recall that if one is interested in the case with no tumbling state then, taking the limit $\beta_0 \to \infty$ one gets $B = 1$.) The other quantities are then given by

$$
\begin{aligned}
a_k &= -\frac{B}{\frac{k^2\pi^2}{L^2} + (2\lambda_0 + 1)B} b_k \\
&\begin{cases} b_1 = \frac{A\pi}{2L} c_2 - c_0 \\ b_k = \frac{A\pi}{2L}(c_{k+1} - c_{k-1}) \quad \text{for } k \geq 2 \end{cases}
\end{aligned}
$$

For Keller-Segel solutions, the k^2 term is absent in the denominator and the result is

$$
\begin{aligned}
c_1 &= \frac{Ab}{2\lambda_0 + 1}(2c_0 - c_2) \\
kc_k &= \frac{Ab}{2\lambda_0 + 1}(c_{k-1} - c_{k+1})
\end{aligned}
\tag{A.2}
$$

For the Keller-Segel equations, $c_k \sim (\alpha_K)^k/k!$ and for L large the moment flux equations have the same behavior, while $k^2\pi^2 = o(L)$ and $c_k \sim (\alpha_F)^k/(k!)^3$ for $L = o(k^2\pi^2)$. (In reality, for the moment flux equations, we are interested in the total population $\rho = n + m = \frac{2\lambda_0+\beta_0}{\beta_0} n + \frac{2b}{\beta_0} n^{0,1}$, which again may be expressed as a Fourier expansion in terms of c_k alone.) This indicates that the moment flux model solution is much smoother than the Keller-Segel one (explaining the higher peaks of Keller-Segel solutions) and that, if L is small, the solutions

differ completely. Figure A.9 shows the results of both the tumbling and finite excitation time models for such a form of $g(S)$.

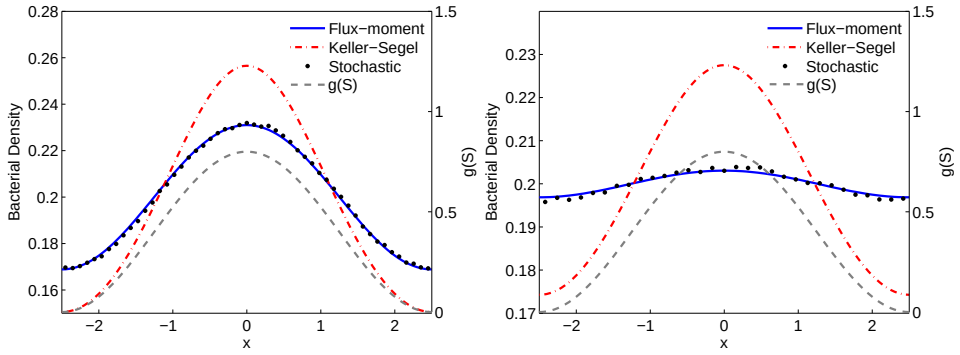

(a) Tumbling, $\beta_0 = 1$.

(b) Excitation, $\tau = 0.5$.

Figure A.9: Moment flux models for Fourier Expansion. $\lambda_0 = 1, a = 0.4, b = 1, A = 0.4$ and $g(S) = \frac{A}{\pi a}(1 + \cos(\pi a x))$

References

[1] ADLER, J., A method for measuring chemotaxis and use of the method to determine optimum conditions for chemotaxis by Escherichia coli. J. Gen. Microbiol. 74 (1973), pp. 7791.

[2] BERG, H. and D. BROWN, Chemotaxis in Escherichia coli analyzed by three-dimensional tracking, Nature, 239 (1972): pp. 500-504.

[3] BUDRENE, ELENA O. and H.C. BERG, Complex patterns formed by motile cells of Escherichia coli, Nature, 349 (1991): pp. 630 - 633.

[4] BLOCK, STEVEN M, SEGALL, JEFFREY E., BERG, H.C., Adaptation kinetics in bacterial chemotaxis, J. Bact., 154 (1983): pp. 312-323.

[5] BRAY, D., LEVIN, M.D., and K. LIPKOW, The chemotactic behavior of computer-based surrogate bacteria, Current Biology, 17 (2007): pp. 12-19.

[6] CHALUB, F.A.C.C., MARKOWICH, P.A., PERTHAME, B., SCHMEISER, C., Kinetic Models for Chemotaxis and their Drift-Diffusion Limits, Monatshefte fr Mathematik, 142 (2004): pp. 123-141.

[7] ERBAN, R. and H.G. OTHMER, From individual to collective behavior in bacterial chemotaxis, SIAM J. Appl. Math, 65 (2004): pp. 361-391.

[8] ERBAN, R. and H.G. OTHMER, From signal transduction to spatial pattern formation in E. coli: a paradigm for multiscale modeling in biology, Multiscale model. simul., 3 (2005): pp. 362-394.

[9] KELLER, E. and L. SEGEL, Model for chemotaxis, J. Theor. Biol., 30 (1971): pp. 225-234.

[10] MITTAL, N, BUDRENE, E.O., BRENNER, M.P., VAN OUDENAARDEN, A., Motility of Escherichia coli cells in clusters formed by chemotactic aggregation, PNAS, 100 (2003): pp. 1325913263.

[11] TINDALL, M.J., MAINI, P.K., PORTER, S.L., ARMITAGE, J.P., Overview of mathematical approaches used to model bacterial chemotaxis II: bacterial populations, Bull. Math. Biol., 70 (2008): pp. 1570-1607.

[12] TYSON, R., LUBKIN, S.R. and J.D. MURRAY, A minimal mechanism for bacterial pattern formation, Proceedings of the Royal Society of London B., 266 (1999): pp. 299-304.